Chemistry Research Journal, 2025, 10(2):35-46
Available online www.chemrj.org

Research Article

ISSN: 2455-8990
CODEN(USA): CRJHA5

Supercapacitor Electrode Fabricated by Activated Carbon Obtained from Peels of Sunflower Seeds (*Helianthus annuus* L.)

Mohamed S. El-Hofy[1], Shaker Ebrahim[3], Alaa E. Ali[1], Gehan S. Elasala[1], Abdel-Hamed Sakr[2]

[1]Chemistry Department, Faculty of Science, Damanhur University, Damanhour, Egypt
[2]Physics Department, Faculty of Science, Damanhour University, Damanhour, Egypt
[3]Department of Materials Science, Institute of Graduate Studies and Research, Alexandria University, Alexandria, Egypt

Abstract

Peels of sunflower seeds (*Helianthus annuus* L.) are used to prepare an activated carbon, AC, which is characterized by different tools (FTIR, Raman, BET, EDX, XRD, SEM and TEM). FTIR spectra shows a variety of functional groups, including hydroxyl, alkyl, carbonyl, and possibly alkyne groups. All these groups influence the adsorption properties and surface reactivity of the prepared AC. Raman spectroscopy indicated the combination of disordered carbon structures with some degree of graphitization. BET analysis showed that the surface area of the AC is 870.959 m2/g. BJH pplot, poresize distribution proved that a significant volume of the material has micropores (pores less than 2 nm) and mesopores (pores between 2 nm to 50 nm) and a very small volume of material has macropores (pores larger than 50 nm). The isotherm plot proved that the sample is the combination of Type I and Type IV, indicating both micropores and mesopores present in the samples. EDX showed that the sample consists entirely of C, O and K, with no trace of any contaminants or precursor residues. The combination of amorphous and semi crystalline structure is proved by XRD. SEM analysis study proved a nano sized, spherical and porous particle. TEM elucidated the morphology looks somewhat amorphous and non-uniform.

The electrochemical characterization was performed by cyclic voltammetry, CV, and galvanostatic charge-discharge, GCD, test in 6 M KOH electrolyte. The AC from peels of sunflower seeds could be a promising low-cost electrode material for supercapacitors where AC electrode obtained a specific capacitance of 209.17 Fg^{-1} at 0.5 Ag^{-1}.

Graphical Abstract

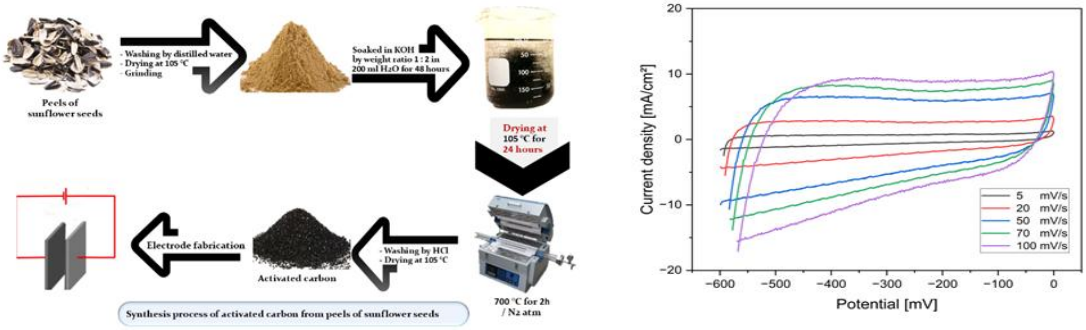

Keywords: Activated carbon; Sunflower Seeds; *Helianthus annuus* L.; Supercapacitor Electrode; Electrochemical

1. Introduction

Severe environmental pollution, expeditious fossil fuels consumption, and fast expansion of sustainable economy worsening the ecological conditions for human survival as well as generating energy depletion [1], [2], [3], [4]. Therefore, a device needs to be developed that might have low pollution concerns, cost effective and produce renewable energy to overcome the energy crisis concern [5], [6]. Renewal of electrical energy as alternative energy in replacing fossil fuels is the solution to this problem, so it takes an energy storage medium that has a large power density and energy density so that it can store energy on a large scale and has a short charging time and its use in the long term, for a long time, one of the alternative energy devices that can be used is a supercapacitor [6].

Supercapacitors, electrochemical or ultra-capacitors have emerged as promising energy storage devices due to their unique characteristics and advantages [7], [8], [9], [10], [11]. Supercapacitors combine the deficiencies of batteries and capacitors, offering high power density, rapid charge-discharge rates and exceptional cyclability, making them well-suited for numerous applications [12]. This makes them a potential candidate to alleviate challenges posed by the excessive utilization of fossil fuels. Supercapacitors, based on their energy-storing mechanisms, are classified into electric double-layer capacitors (EDLCs) and pseudocapacitors. The former stores energy by separating charge in Helmholtz double-layer across the interface of electrodes and electrolytes [13] whereas the latter use electro sorption, reduction-oxidation reactions, and intercalation processes to store energy [14].

Supercapacitors consist of electrodes, electrolyte, current collector, and separator. The electrode is one of the factors that affect the effectiveness of the supercapacitor. Electrodes can be made of polymers, metal oxides, and AC. Polymers and metal oxides are less stable, have relatively low conductivity, high production costs, and are scarce, so that AC derived from biomass is used as a substitute [15], [16]. AC derived from biomass for supercapacitor cell electrodes has characteristics such as being environmentally friendly, relatively inexpensive, and the availability of abundant materials. Various types of biomasses have been used as raw materials for AC including the following cattails [16], barley straw [17],[18], rubber seed shells [18], hybrid willow [19], banana [20] and in this study used peel of sunflower seed kernels biomass.

There are more than 70 species of sunflowers (*Helianthus annuus* L.), an annual, short-season herbaceous crop in the Asteraceae family, known worldwide [21]. In Egypt, it is commonly available. It is distinguished by a characteristic huge, round, yellow flower head inflorescence that faces the light directly and bears achenes that mature into seeds [21], [22]. Sunflower seeds are used to make oil and as food. Protected by a hull up to 21_30% of seed weight [22]and a 12 mm thick sunflower hull with a dark brown and rough exterior. Sunflower seed hull waste is underutilized as a substitute carbon source for natural antioxidants and beneficial biopolymers for materials, dietary fibers, additives or food preservation elements [23]. The content of the sunflower hull is almost 30% cellulose, 26.4% lignin, 38.5% of neutral sugars, mainly hemicelluloses, and only 1.3% of proteins [23]. In this research, we prepare the AC material from peel of sunflower seeds for supercapacitor electrodes which makes it useful and has high economic value.

2. Materials and Methods

Materials

Peels of sunflower seeds were supplied from an Egyptian market. Potassium hydroxide (KOH) was obtained from PIOCHEM company. HCl (30%) from EL SALAM FOR CHEMICAL INDUSTRY was purchased. Carbon black and polyvinylidene difluoride (PVDF) powder was received from Alfa Aesar. N-methyl-2-pyrrolidone (NMP) (99%) was received from Alfa Aesar. Graphite sheet with carbon ratio more than 99.5%, density of 1.1 g/ cm3 and thickness of 0.3 mm was purchased from XRD carbon, China.

AC Synthesis

Peels of sunflower seeds were gathered from the local market, and these raw materials were washed with distilled water several times, dried at 105 °C for 24 h, and then grinded to powder. After grinding, the alkali treatment was carried out by dipping the sample in a beaker containing KOH (1:2 by weight) in 200 mL of water for 48 hours. Then the mixture was dried at 105 °C for 24 h and then placed into a tube furnace for 2 h at 700 °C as shown in

Figure 1. The carbonization processes were operated under a nitrogen atmosphere (100 mL min^{-1}) with a heating rate of 5 °C min^{-1}. The samples in the furnace were cooled to room temperature, and then the samples were rinsed with 1.0 M HCl to remove any inorganic impurities and then washed with deionized water. Finally, the AC obtained was dried at 105 °C for 12 h in the oven [24].

Electrode Fabrication

The electrode was prepared by depositing the slurry of the active material over the Graphite sheet. A slurry was prepared by mixing the active material (AC), carbon black, polyvinylidene fluoride (PVDF), binder with the ratio of 80:10:10 and N-Methyl pyrrolidone (NMP) was used as solvent. The slurry was put over the magnetic stirrer 24 h [25]. Furthermore, the prepared slurry was deposited over the Graphite with the help of micropipette and kept in oven for 12 h at 60 °C to dry. The weights of the substrate before coating and after the heating were determined to achieve the weight of electroactive material on it.

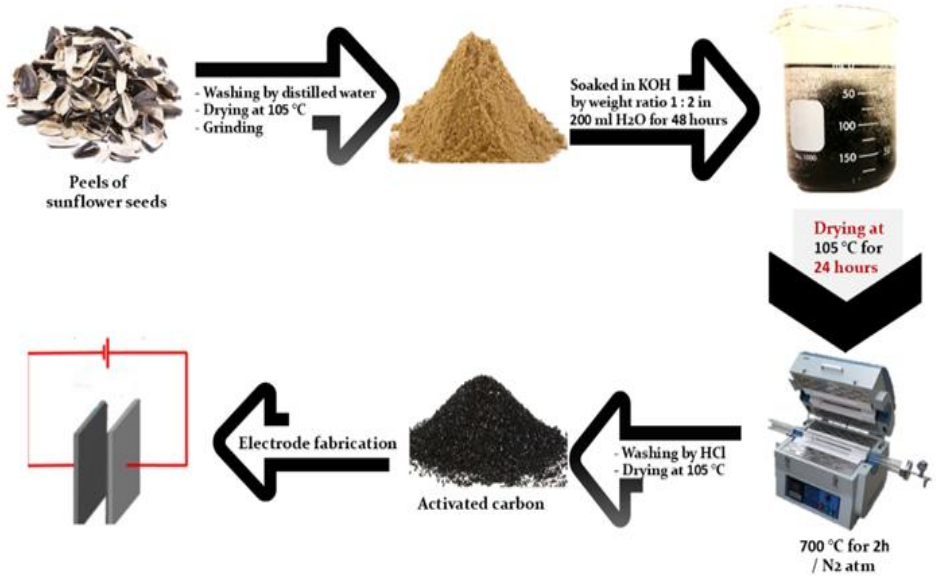

Figure 1: Synthesis process of AC from peels of sunflower seeds.

Characterization and Measurements

The study of the surface morphology of the AC was carried out using scanning electron microscopy (SEM) and transmission electron microscopy (TEM). Its elemental composition was determined by using Signal SED, Landing Voltage ,20.0 kV, WD 10.0 mm, Magnification x120, Vacuum Mode High Vacuum (Edx). The structural properties were studied by XRD analysis using the Bruker X-ray powder diffraction -XRD-D2 phaser instrument made in Germany, with Cu Kα (λ = 1.54 Å) as a radiation source and the 2θ scan angle from 10 to 100 °. Raman spectroscopy was used to determine the relative disorder of carbons in the sample by Confocal Raman microscope (Witec,300R alpha R, made in Germany) Laser source 532 nm. The Fourier transform infrared (FTIR) analysis was conducted using FT/IR-4600 spectrometer. The N2 adsorption/desorption isotherms, surface area and pore size distributions of the sample were measured using BET analysis (BELSORP-miniX). CV, GCD, and EIS tests were performed by OrigaFlex-OGF05 (Origalys, France). Using a three-electrode system consisting of a graphite sheet as the working electrode (WE), a platinum plate as the counter electrode (CE), and Ag/AgCl as the reference electrode (RE), all experiments were conducted in 6 M KOH aqueous electrolyte solutions.

The following formulas were used to determine the specific capacitance (Cs) value in the three-electrode configuration from the GCDs and CV plots [26]:

$$Cs\ (F/g) = \frac{I\ *\ \Delta t}{m\ *\ \Delta V} \qquad (1)$$

$$Cs = \frac{\int I \ * dV}{\nu * m * V} \qquad (2)$$

where, Δt is the discharge time (s), I (A) is the applied current, ΔV (V) is the applied potential, ν is the scan rate, and m (g) is the mass of the electrode material on a graphite sheet.

Furthermore, it was thought that two important parameters for the suitability of electrode material in a SC were specific energy and power, and they were estimated by the following equations [26]:

$$E\ (W\ h/Kg) = \frac{1}{7.2} * Cs * \ V^2 \qquad (3)$$

$$P(W/Kg) = \frac{E}{\Delta t} * 3600 \qquad (4)$$

where E is the specific energy ($Wh \cdot kg^{-1}$), P is the specific power ($W \cdot kg^{-1}$), I is the specific current ($A \cdot g^{-1}$), t is the discharge time (s) and V is the potential window of the symmetric device.

3. Results and Discussion

Structural properties of AC prepared from peels of sunflower seeds

FTIR spectra showed that the AC contains a variety of functional groups, such as hydroxyl, alkyl, carbonyl, and potentially alkyne groups. These groups facilitate the adsorption properties and surface reactivity of AC. A broad peak, Fig. 2, indicated hydroxyl groups is observed at approximately 3441 cm^{-1}, which is the stretching vibration of the O-H bond [27]. There are carbonyl groups present because the C=O bond's stretching vibration is assigned at about 1731 cm^{-1}. The stretching vibration of the C=C bond is represented by the peak at 1637 cm^{-1}. However, the transmit peaks at 1123–1047 cm^{-1} are attributed to the C-O bond, suggesting that ether, alcohol, or ester groups are present. The fingerprint region for different bending vibrations, such as C-H, C-C, or C-O bonds, is between 875 and 411 cm^{-1}. The presence of alkane structures is indicated by the appearance of the C-H bending vibration bond at about 1383 cm^{-1}. This demonstrates how the C=O can be changed into other oxygen-containing functional groups by KOH activation. These results indicate that the KOH activation can generate ether functional groups on the AC. Ion transport in the AC nanometre and sub-nanometre pores is thought to be facilitated by the hydrophilic surface that the OH groups on the AC can provide [28].

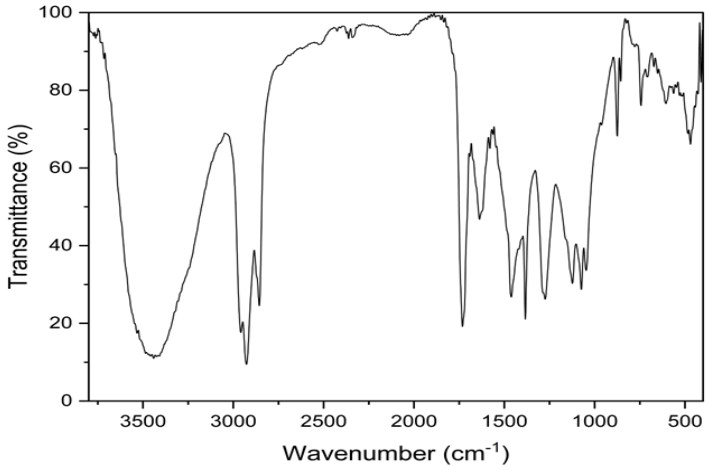

Figure 2: FTIR spectrum of AC prepared from peels of sunflower seeds.

The carbonization which measures the ordered carbon structure, and the disordered structure are both examined by Raman spectroscopy which showed that the AC had the two distinct characteristic peaks (D and G bands) of typical AC, Fig. 3. A lattice breathing mode of sp^3 carbon bond vibration is typically attributed to the D band at approximately 1361 cm^{-1} when the AC has structural disorder [27]. The D-band shows how many defects in structure there are in the carbon material. This structural disorder might be contributed to by the functional groups

on graphitic sheets that contain oxygen [28]. The stretching of the bonds between two sp^2 hybridized carbon atoms in the AC is represented by the G band, which is located at about 1580 cm^{-1} [29]. The I_D/I_G ratio of the AC is 0.93, indicating that AC is largely made of carbon structure with high porosity, more defective sites, and an ordered graphitic feature [30]. The rise in the I_D/I_G ratio in the AC indicates the increase in the degree of disorder in the carbon material, which is in agreement with the XRD result [31]. The presence of some oxygen-containing functional groups or other structural irregularities may be indicated by the broad and small peaks in the higher wavenumber region, which is located at approximately 2927 cm^{-1}. For ion adsorption and electrochemical reactions, disordered carbon performs the role of an active site, while ordered graphitic layers offer good electrical conductivity but decrease active sites [32], [33].

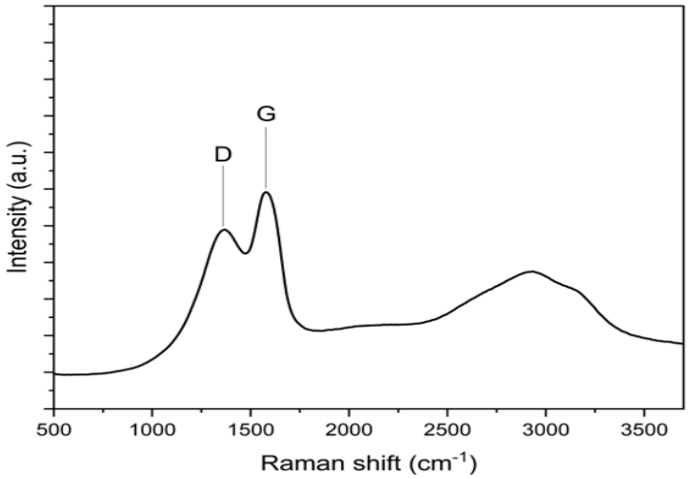

Figure 3: Raman spectrum of AC prepared from peels of sunflower seeds.

The crystalline properties of the AC are investigated by XRD, where the XRD pattern, Fig. 4, of the AC showed two sharp characteristics of peaks at 17.7° and 26° corresponding to the (220) and (002) crystal lattice planes, respectively [28], [34]. The presence of other small peaks at 40° and 52° is due to the impurities. In addition, some peaks are attributed to anatase potassium oxide due to the material is activated by potassium hydroxide. Typically, the XRD pattern shows that the AC has a combination of semicrystalline and amorphous structure like the data obtained from Raman spectra. The AC porous structure and micropores were formed because of the reaction between KOH and the carbonized sample during the chemical activation [32].

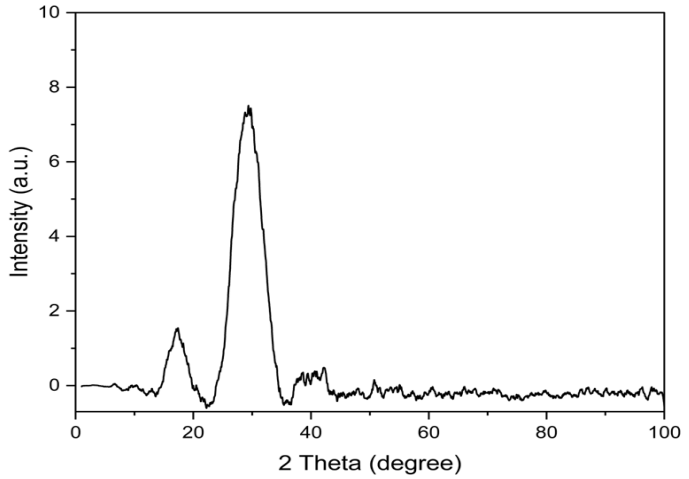

Figure 4: The XRD pattern of AC prepared from peels of sunflower seeds.

Morphological and composition properties of AC prepared from peels of sunflower seeds

The surface morphology of the AC is assisted through SEM as described in Fig. 5(a). The micrographs clearly elucidate nano-sized spherical and homogenous nanoparticles. These nanoparticles are closely together throughout the whole surface. The AC has a porous and irregular structure due to the KOH activation as displayed in Fig. 5(b) [35]. TEM image illustrated in Fig. 5. (c). indicates an agglomeration of the AC nanoparticles due to the electrostatic charges. These nanoparticles have a size of nearly 17–24 nm, as described in Fig. 5(d). According to the images, AC contains mesopores and micropores, which facilitate faster charge transport and enhance electrolyte ion transport [36]. The difference in size of AC obtained from SEM and TEM is attributed to the methods of sample preparation where SEM shows larger sizes due to surface morphology analysis and agglomeration effects, while TEM provides more accurate internal structure and real particle sizes or grain sizes due to its higher resolution and thin sample preparation. Carbon is the main chemical component found in AC. Oxygen may be present because of oxygen-containing functional groups in the AC and water vapour that has been absorbed from the air. The organic nature of the precursor accounts for additional elemental traces [34]. As shown in Fig. 5(e), EDX characterisation is used to conduct an elemental analysis of the produced AC. We discovered that the sample is completely composed of C, O, and K; no impurities or precursor residues were detected.

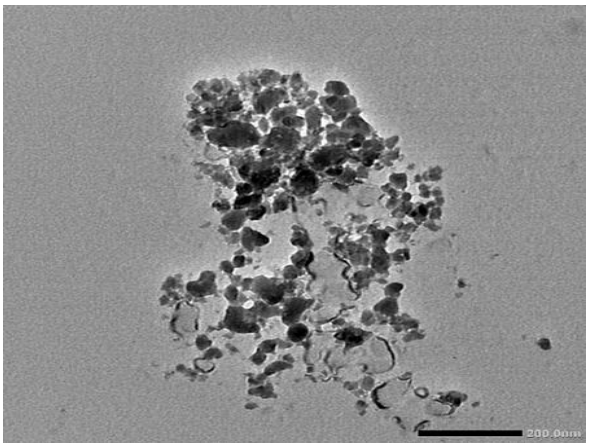

(a)

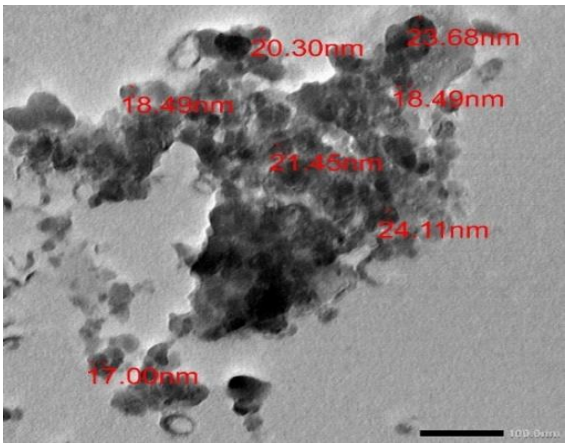

(b)

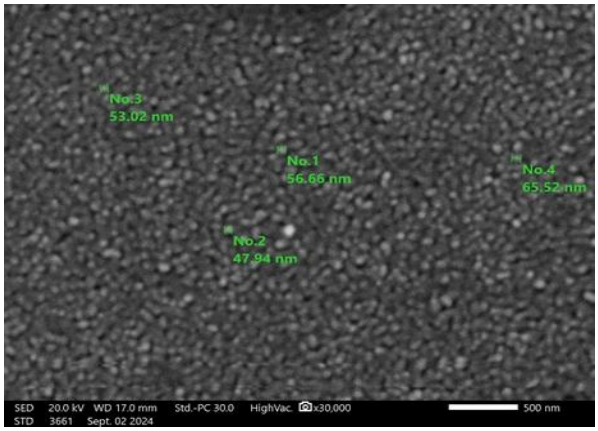

(c)

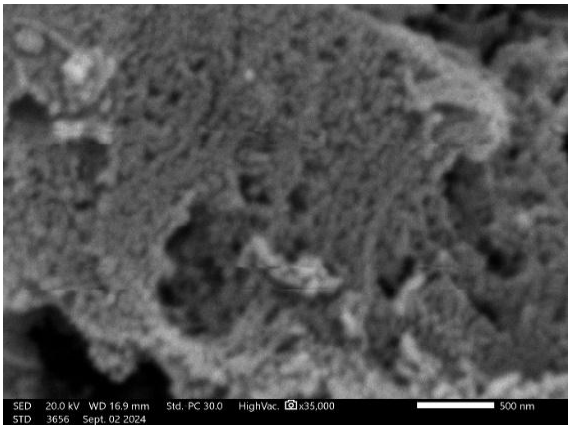

(d)

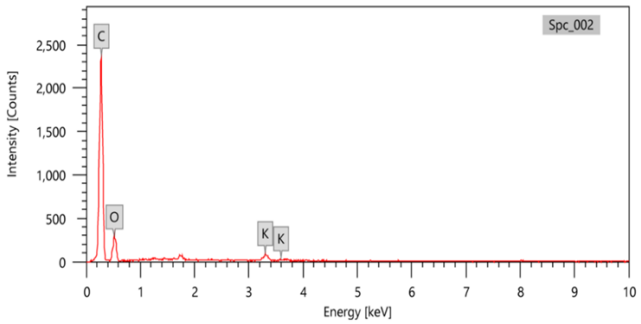

(e)

Figure 5: SEM (a, b), TEM (c, d) images, and EDX (e) spectrum of AC prepared from peels of sunflower seeds.

Porosity properties of AC prepared from peels of sunflower seeds.

To explore the surface area of the synthesized AC, a nitrogen adsorption/desorption characterization was performed. The Brunauer-Emmett-Teller (BET) analysis reveals that the surface area of AC is 870.959m^2/g. Fig. 6(a) depicts the pore size distribution, BJH plot, and nitrogen adsorption/desorption isotherm of AC [28]. It indicates that a significant volume of the material has micropores (pores less than 2 nm) and mesopores (pores between 2 nm to 50 nm), and a very small volume of material has macropores (pores larger than 50 nm) [34], [37]. The BJH plot shows that the AC has a significant number of small pores, which is typical for materials with a high surface area used in adsorption processes.

The adsorption/desorption isotherm plot has a small increase in the adsorbed volume as shown in Fig. 6(b), which corresponds to the monolayer adsorption phase ($P/P_0 < 0.1$), which is typical of microporous materials. As pressure increases (approximately $P/P_0 \approx 0.2$ to 0.4), the adsorbed volume rises more noticeably. This region represents multilayer adsorption as more layers of adsorbate molecules form on top of the initial monolayer. As pressure increases (approximately $p/p_0 > 0.4$), the adsorbed volume increases sharply due to capillary condensation. The isotherm is identified as the combination of Type I and Type IV, indicating both micropores and mesopores present in the ACs [27], [30]. This reflects a combination of monolayer and multilayer adsorption followed by capillary condensation, characteristic of mesoporous materials.

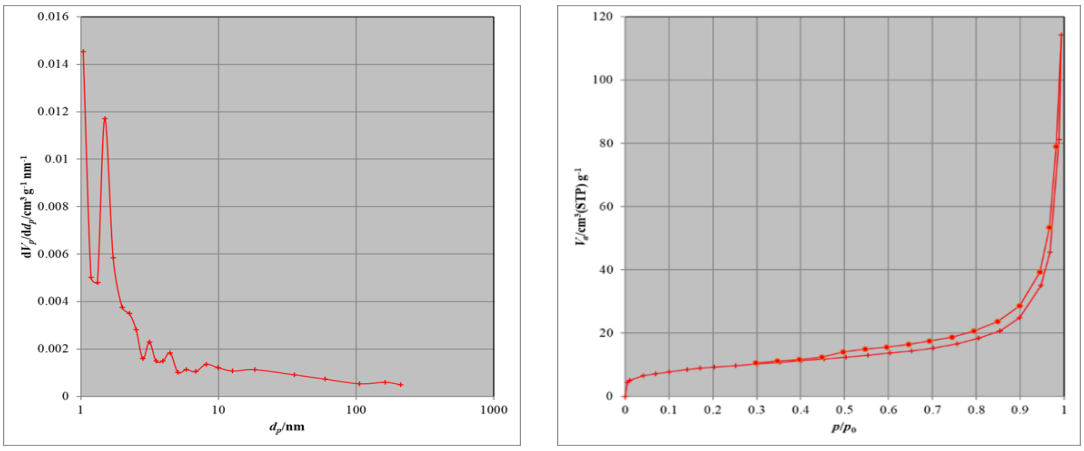

(a) *(b)*

Figure 6: Pore size distribution obtained (BJH) (a) and Nitrogen adsorption-desorption isotherm (b).

Electrochemical properties

The CV technique evaluates capacitive properties, subsequently demonstrating the relationship between current density and voltage window. The CV curves, Fig. 7, of the AC exhibited a quasi-rectangular shape with no redox

peak [38] that is the characteristic of the electrical double-layer capacitor (EDLC). Also, even at a high scan rate of 100 mVs-1, CV curves maintain the characteristic rectangular shape, indicating good charge transfer ability. The specific capacitance at scan rates of 5, 20, 50,70 and 100 mVs-1 are 122.34, 120.97, 105.56, 91.50 and 72.76 Fg -1 , respectively. This result shows a reduction in specific capacitance with increasing scan rate because the ions have enough time to diffuse through the surface of the micropores at slow scan rates. But at a high scan rate, the ions require pores with a larger size to enter the AC surface, and a small active surface area of the pores can be utilized, thus the micropores of AC store the charges, while mesopores can be accessed with the fast of ions.

In addition, this confirmed the appearance nanosized structure of samples, due to the opening of pores in combination of micropores and mesopores. This corresponds to the turbostratic (disordered) structures of AC found in the sample, as confirmed in a XRD analysis.

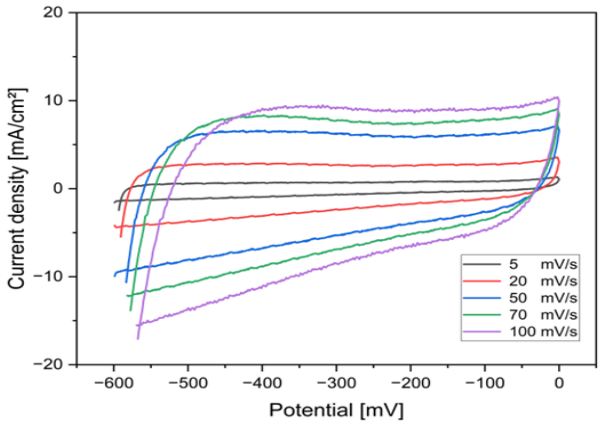

Figure 7: CV curve of AC prepared from peels of sunflower seeds electrode at different scan rates in 6 M KOH.

GCD curves, Fig. 8, shows the relation between potential and time at various current densities. The specific capacitance value of this electrode of the peel of a sunflower seed-based AC at 0.5, 1, 1.5, 2, 2.5, and 3 A g-1 are 209.17, 168.33, 156.25, 149.00, 146.67, and 142.00 F g^{-1}, respectively. There is a reduction in the specific capacitance value as the current density is increased from 1 to 3 A g-1 indicating high capacitive performance during the rapid charge and discharge process. This is due to the presence of both micropores and mesopores in the AC, as indicated by the BJH plot. All of the curves in the charge and discharge regions preserve their linear shapes, indicating capacitive behavior, and hence confirm the double layer formation on the electrode-electrolyte interface. The internal resistance drop is also very small, indicating small internal resistance and hence low energy dissipation of the capacitor [39].

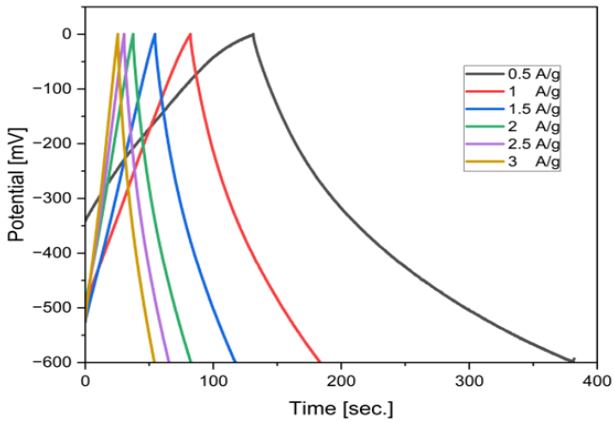

Figure 8: GCD curves of AC prepared from peels of sunflower seeds electrode at different current densities.

EIS analyzes the impedance of super capacitor electrodes, where in an alternating potential with changing frequency is applied [40]. The measurement can be used to evaluate electrochemical interfacial parameter SCs, such as series resistance, charge transfer resistance, and diffusion control (sometimes called the Warburg effect from the porous structure of the electrode material). EIS is conducted at the open circuit voltage (OCV) by applying a small amplitude of alternative potential (5 mV) in a range of frequency from 0.05 to 10 kHz. Fig. 9 illustrates the obtained Nyquist plots. It can be seen that the Nyquist plots consisted of a small semicircle at a high-frequency region and a spike 45° inclined to the x-axis. The presence of the spike 45° inclined to the x-axis is characteristic of a capacitor. The Nyquist plot obtained could be the best fit with the Randles circuit shown in the inset of Fig. 9. The equivalent circuit consists of a solution resistance (R_s = 2.35 Ω), charge transfer resistance (R_{ct} = 15.65 Ω), and double-layer capacitance (C_{dl}= 1.02 mF) in parallel with the Warburg component (W = 20.48 Ω $s^{-1/2}$).

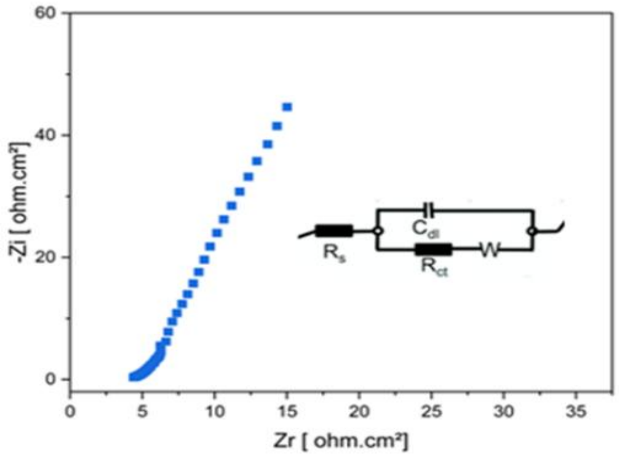

Figure 9: Nyquist plots recorded for AC from peels of sunflower seeds, inset: Equivalent circuit used for fitting the Nyquist plot.

4. Conclusion

In this research, low-cost AC derived from peels of sunflower seeds (*Helianthus annuus* L.) was successfully prepared using the carbonization process under N2 and used as SC electrode, characterized by FTIR, Raman, BET, EDX, XRD, SEM and TEM. FTIR spectrum to indicate that the prepared AC contains a variety of functional groups. Raman spectra indicated that the AC has disordered carbon structures. XRD pattern proved that the AC is amorphous. SEM and TEM proved nanosized, spherical, and porous particles with amorphous and non-uniform morphology. The carbon percent was found to be 72.92 from the EDX diagram. BET analysis gives a large surface area with micropores and mesopores in nature. The isotherm plot proved that the AC is a combination of Type I and Type IV, indicating both micro- and mesopores present in the ACs. The AC electrode produced a specific capacitance of 209.17 F g^{-1} at 0.5 Ag^{-1}. Thus, AC from peels of sunflower seeds could be a promising low-cost electrode material for SCs.

Declaration of Competing Interest

The authors declare that they have no known competing financial interests or personal relationships that could have appeared to influence the work reported in this paper

Acknowledgments

"This paper is based upon work supported by Science, Technology & Innovation Funding Authority (STDF) under grant".

References

[1]. W. Qiu et al., "Phosphate ion and oxygen defect-modulated nickel cobaltite nanowires: a bifunctional cathode for flexible hybrid supercapacitors and microbial fuel cells," J Mater Chem A Mater, vol. 8, no. 17, pp. 8722–8730, May 2020, doi: 10.1039/d0ta01423k.

[2]. J. Wei, X. Li, H. Xue, J. Shao, R. Zhu, and H. Pang, "Hollow Structural Transition Metal Oxide for Advanced Supercapacitors," May 09, 2018, Wiley-VCH Verlag. doi: 10.1002/admi.201701509.

[3]. L. Liu et al., "Synthesis of self-templated urchin-like $Ni_2Co(CO_3)_2(OH)_2$ hollow microspheres for high-performance hybrid supercapacitor electrodes," Electrochim Acta, vol. 327, Dec. 2019, doi: 10.1016/j.electacta.2019.134970.

[4]. M. Z. Iqbal, M. M. Faisal, S. R. Ali, S. Farid, and A. M. Afzal, "Co-MOF/polyaniline-based electrode material for high performance supercapattery devices," Electrochim Acta, vol. 346, Jun. 2020, doi: 10.1016/j.electacta.2020.136039.

[5]. A. Noori, M. F. El-Kady, M. S. Rahmanifar, R. B. Kaner, and M. F. Mousavi, "Towards establishing standard performance metrics for batteries, supercapacitors and beyond," Mar. 07, 2019, Royal Society of Chemistry. doi: 10.1039/c8cs00581h.

[6]. T. Subramaniam, M. A. M. Nainar, and N. A. Nordin, "A Review on Synthesis and Characterization of Activated Carbon from Natural Fibers for Supercapacitor Application," Jan. 01, 2022, Universiti Putra Malaysia Press. doi: 10.47836/pjst.30.1.20.

[7]. M. A. Dar, D. Govindarajan, and G. N. Dar, "Facile synthesis of SnS nanostructures with different morphologies for supercapacitor and dye-sensitized solar cell applications," Journal of Materials Science: Materials in Electronics, vol. 32, no. 15, pp. 20394–20409, Aug. 2021, doi: 10.1007/s10854-021-06550-w.

[8]. M. A. Dar, D. Govindarajan, K. M. Batoo, and C. Siva, "Supercapacitor and magnetic properties of Fe doped SnS nanoparticles synthesized through solvothermal method," J Energy Storage, vol. 52, Aug. 2022, doi: 10.1016/j.est.2022.105034.

[9]. M. A. Dar, D. Govindarajan, K. M. Batoo, M. Hadi, and G. N. Dar, "Photovoltaic and Supercapacitor performance of SnSe nanoparticles prepared through co-precipitation method," Materials Technology, vol. 37, no. 10, pp. 1396–1409, 2022, doi: 10.1080/10667857.2021.1950887.

[10]. M. Arif Dar, M. Y. Bhat, N. Ahmad Mala, H. Ahmad Rather, S. Venkatachalam, and N. Srinivasan, "Structural, morphological and supercapacitor applications of SnS nanomaterials prepared in three different types of solvents," in Materials Today: Proceedings, Elsevier Ltd, Jan. 2022, pp. 1689–1698. doi: 10.1016/j.matpr.2022.05.264.

[11]. M. A. Dar, D. Govindarajan, and G. N. Dar, "Comparing the Electrochemical Performance of Bare SnS and Cr-Doped SnS Nanoparticles Synthesized through Solvothermal Method," Physics of the Solid State, vol. 63, no. 9, pp. 1343–1350, Sep. 2021, doi: 10.1134/S1063783421090055.

[12]. S. Thomas, A. B. Gueye, and R. K. Gupta, Eds., Nanostructured Materials for Supercapacitors. in Advances in Material Research and Technology. Cham: Springer International Publishing, 2022. doi: 10.1007/978-3-030-99302-3.

[13]. D. Qu and H. Shi, "Studies of activated carbons used in double-layer capacitors," 1998.

[14]. B. E. Conway, V. Birss, and J. Wojtowicz, "The role and utilization of pseudocapacitance for energy storage by supercapacitors," 1997.

[15]. R. Srinivasan et al., "Sustainable porous activated carbon from Polyalthia longifolia seeds as electrode material for supercapacitor application," Journal of Electroanalytical Chemistry, vol. 849, Sep. 2019, doi: 10.1016/j.jelechem.2019.113382.

[16]. M. Yu, Y. Han, J. Li, and L. Wang, "CO2-activated porous carbon derived from cattail biomass for removal of malachite green dye and application as supercapacitors," Chemical Engineering Journal, vol. 317, pp. 493–502, 2017, doi: 10.1016/j.cej.2017.02.105.

[17]. J. Pallarés, A. González-Cencerrado, and I. Arauzo, "Production and characterization of activated carbon from barley straw by physical activation with carbon dioxide and steam."

[18]. R. Farma, H. Husni, I. Apriyani, A. Awitdrus, and E. Taer, "Biomass Waste-Derived Rubber Seed Shell Functionalized Porous Carbon As an Inexpensive and Sustainable Energy Material for Supercapacitors," J Electron Mater, vol. 50, no. 12, pp. 6910–6919, Dec. 2021, doi: 10.1007/s11664-021-09226-7.

[19]. C. Jiang, G. A. Yakaboylu, T. Yumak, J. W. Zondlo, and J. Wang, "Activated Carbons Prepared by Indirect and Direct CO2 Activation of Lignocellulosic Biomass for Supercapacitor Electrodes 2," 2020.

[20]. E. Lei, W. Li, C. Ma, Z. Xu, and S. Liu, "CO 2 -activated porous self-templated N-doped carbon aerogel derived from banana for high-performance supercapacitors," Appl Surf Sci, vol. 457, pp. 477–486, Nov. 2018, doi: 10.1016/j.apsusc.2018.07.001.

[21]. B. S. Adeleke and O. O. Babalola, "Oilseed crop sunflower (*Helianthus annuus*) as a source of food: Nutritional and health benefits," Sep. 01, 2020, Wiley-Blackwell. doi: 10.1002/fsn3.1783.

[22]. T. J. Gulya, "SUNFLOWER." [Online]. Available: www.sunflowernsa.org.

[23]. M. D. De'Nobili, D. C. Bernhardt, M. F. Basanta, and A. M. Rojas, "Sunflower (*Helianthus annuus* L.) Seed Hull Waste: Composition, Antioxidant Activity, and Filler Performance in Pectin-Based Film Composites," Front Nutr, vol. 8, Dec. 2021, doi: 10.3389/fnut.2021.777214.

[24]. V. Hiremath, A. C. Lim, and J. G. Seo, "Highly porous honeycomb-like activated carbon derived using cellulose pulp for symmetric supercapacitors," Int J Energy Res, vol. 45, no. 3, pp. 4385–4395, Mar. 2021, doi: 10.1002/er.6108.

[25]. Y. Yuan et al., "Nitrogen-doped hierarchical porous activated carbon derived from paddy for high-performance supercapacitors," Materials, vol. 14, no. 2, pp. 1–12, Jan. 2021, doi: 10.3390/ma14020318.

[26]. R. Nasser, J. Tiantian, and J. M. Song, "Hierarchical porous activated carbon derived from olives: Preparation, (N, S) co-doping, and its application in supercapacitors," J Energy Storage, vol. 51, Jul. 2022, doi: 10.1016/j.est.2022.104348.

[27]. M. Vinayagam, R. Suresh Babu, A. Sivasamy, and A. L. Ferreira de Barros, "Biomass-derived porous activated carbon from Syzygium cumini fruit shells and Chrysopogon zizanioides roots for high-energy density symmetric supercapacitors," Biomass Bioenergy, vol. 143, Dec. 2020, doi: 10.1016/j.biombioe.2020.105838.

[28]. R. Bi, S. K. Pang, K. C. Yung, and L. K. Yin, "Comprehensive study of used cigarette filters-derived porous activated carbon for Supercapacitors: From biomass waste to sustainable energy source," Journal of Electroanalytical Chemistry, vol. 925, Nov. 2022, doi: 10.1016/j.jelechem.2022.116915.

[29]. V. V. Pavlenko, K. M. Temirkulova, A. Y. Zakharov, Y. A. Aubakirov, and Z. E. Ayaganov, "Optimization of the Porous Structure of Carbon Electrodes for Hybrid Supercapacitors with a Redox Electrolyte Based on Potassium Bromide," Eurasian Chemico-Technological Journal, vol. 25, no. 4, pp. 201–210, 2023, doi: 10.18321/ectj1542.

[30]. M. Vinayagam, R. Suresh Babu, A. Sivasamy, and A. L. F. de Barros, "Biomass-derived porous activated carbon nanofibers from Sapindus trifoliatus nut shells for high-performance symmetric supercapacitor applications," Carbon Letters, vol. 31, no. 6, pp. 1133–1143, Dec. 2021, doi: 10.1007/s42823-021-00235-4.

[31]. S. Sundriyal et al., "Waste Office Papers as a Cellulosic Material Reservoir to Derive Highly Porous Activated Carbon for Solid-State Electrochemical Capacitor," IEEE Trans Nanotechnol, vol. 20, pp. 481–488, 2021, doi: 10.1109/TNANO.2021.3080589.

[32]. W. Sun, Y. Zhang, and F. Yang, "A High-Performance Symmetric Supercapacitor from Porous Activated Carbon under Compression," Energy Technology, vol. 9, no. 5, May 2021, doi: 10.1002/ente.202100068.

[33]. M. Sandhiya, M. P. Nadira, and M. Sathish, "Fabrication of Flexible Supercapacitor Using N-Doped Porous Activated Carbon Derived from Poultry Waste," Energy and Fuels, vol. 35, no. 18, pp. 15094–15100, Sep. 2021, doi: 10.1021/acs.energyfuels.1c01713.

[34]. O. Khadka, U. Lawaju, S. Koju, R. C. Rai, M. L. Nakarmi, and P. Joshi, "Activated carbon derived from coffee waste as supercapacitor electrode material," Scientific World, vol. 17, no. 17, pp. 19–26, Jun. 2024, doi: 10.3126/sw.v17i17.66416.

[35]. R. Bi, S. K. Pang, K. C. Yung, and L. K. Yin, "Comprehensive study of used cigarette filters-derived porous activated carbon for Supercapacitors: From biomass waste to sustainable energy source," Journal of Electroanalytical Chemistry, vol. 925, Nov. 2022, doi: 10.1016/j.jelechem.2022.116915.

[36]. R. Nasser, J. Tiantian, and J. M. Song, "Hierarchical porous activated carbon derived from olives: Preparation, (N, S) co-doping, and its application in supercapacitors," J Energy Storage, vol. 51, Jul. 2022, doi: 10.1016/j.est.2022.104348.

[37]. Y. Yuan et al., "Nitrogen-doped hierarchical porous activated carbon derived from paddy for high-performance supercapacitors," Materials, vol. 14, no. 2, pp. 1–12, Jan. 2021, doi: 10.3390/ma14020318.

[38]. S. B. Dhavale et al., "Nanostructured NiCo2O4 embedded on biowaste derived hierarchical porous activated carbon for high performance symmetric and asymmetric supercapacitor device," J Energy Storage, vol. 72, Nov. 2023, doi: 10.1016/j.est.2023.108820.

[39]. O. Khadka, U. Lawaju, S. Koju, R. C. Rai, M. L. Nakarmi, and P. Joshi, "Activated carbon derived from coffee waste as supercapacitor electrode material," Scientific World, vol. 17, no. 17, pp. 19–26, Jun. 2024, doi: 10.3126/sw.v17i17.66416.

[40]. M. Vinayagam, R. Suresh Babu, A. Sivasamy, and A. L. F. de Barros, "Biomass-derived porous activated carbon nanofibers from Sapindus trifoliatus nut shells for high-performance symmetric supercapacitor applications," Carbon Letters, vol. 31, no. 6, pp. 1133–1143, Dec. 2021, doi: 10.1007/s42823-021-00235-4.